

Learning Test-time Data Augmentation for Image Retrieval with Reinforcement Learning

Osman Tursun, Simon Denman, Sridha Sridharan, Clinton Fookes
SAIVT, Queensland University of Technology
{*w.tuerxun, s.denman, s.sridharan, c.clinton*}@qut.edu.au

Abstract. Off-the-shelf convolutional neural network features achieve outstanding results in many image retrieval tasks. However, their invariance is pre-defined by the network architecture and training data. Existing image retrieval approaches require fine-tuning or modification of the pre-trained networks to adapt to the variations in the target data. In contrast, our method enhances the invariance of off-the-shelf features by aggregating features extracted from images augmented with learned test-time augmentations. The optimal ensemble of test-time augmentations is learned automatically through reinforcement learning. Our training is time and resources efficient, and learns a diverse test-time augmentations. Experiment results on trademark retrieval (METU trademark dataset) and landmark retrieval (Oxford5k and Paris6k scene datasets) tasks show the learned ensemble of transformations is effective and transferable. We also achieve state-of-the-art MAP@100 results on the METU trademark dataset.

1 Introduction

The internal activations of convolutional neural networks (CNNs) pre-trained on ImageNet have demonstrated astounding results on various object retrieval tasks [1,2]. Such activations are termed off-the-shelf CNN features and compared to conventional hand-crafted features, they are more discriminative, compact and accessible. To this end, off-the-shelf CNN features are widely used for object retrieval over or in combination with conventional hand-crafted features.

However, un-altered off-the-shelf features are often not sufficiently robust to adapt to variations including changes in scale, illumination, orientation, color, contrast, deformations, and background clutter [3,4]. Thus image retrieval using such features can fail when these challenges are present, as un-altered off-the-shelf features have no in-built invariances besides translational invariance. This is due to these networks being predominately trained with natural images and light data-augmentation. For example, ResNet [5] was trained with only the simple data augmentations of random-crops and horizontal flips. Therefore, off-the-shelf features are not scale, rotation or contrast invariant. However, transform invariant features are desirable for challenging object retrieval tasks.

Many methods have been proposed to enhance the transform invariance of CNN features for classification and recognition. Those methods incorporate

transform invariance either via special structures or data augmentation, or both. Feature extraction modules (*i.e.*, spatial transformer [6], transform capsules [7], multi-column networks [8]), special filters (*i.e.*, deformable filters [9], transformed filters [10,11] and special pooling [4,10,12]) are types of neural structures to improve the transform invariance of neural networks. Generally, these models require training or are only valid for certain datasets or transformations (*i.e.*, scale or rotation), and so lack generality. By comparison, data augmentation is a simple but effective way to achieve transform invariance as only extra transformations on input images are necessary at the training or inference stage. This allows the generation of a more robust descriptor from multiple transformed samples, and the cost of data augmentation can be minimised by parallelization.

In this work, we propose an ensemble approach that increases the invariance of off-the-shelf DCNN features by aggregating features extracted from images with an ensemble of test-time augmentations (TTA). The ensemble of TTA increases the invariance of off-the-shelf features without sacrificing their compactness and discriminability, which is the key to the approach.

Finding the optimal ensemble of TTA is a discrete search problem. Random, grid and heuristic searching are possible solutions, but are expensive and impractical. Reinforcement learning based searching has been widely used for discrete search problems [13,14] such as neural architecture search (NAS) [13]. We, therefore, applied a reinforcement learning based search to find the best ensemble of TTA to extract invariant features for image retrieval. Usually, neural hyper-parameter search and NAS with reinforcement learning requires enormous computational resources, and is time-consuming. To overcome this, we avoid the repeated deep feature extraction process by reusing transformed features through caching. Our proposed reward function learns an ensemble of image transformations that increases both invariance and distinctiveness of features.

Our experimental results on trademark (METU trademark [15] dataset) and landmark retrieval ([16] and Paris6k [17] datasets) tasks show the learned ensemble of image transformations increases the performance of off-the-shelf features. The learned transformation demonstrates its transferability to off-the-shelf features from different pre-trained networks, and is applicable to various aggregation methods. We have achieved the state-of-the-art MAP results on the challenging METU trademark dataset with the learned ensemble of TTA.

2 Related Efforts

Test-time augmentation has been widely used by image recognition and retrieval tasks [4,18,19,20] due to its effectiveness. Multi-cropping and horizontal-flipping are applied for testing AlexNet [18], VGG16 [19], ResNet [5], and Inception [20] models. Multi-scale cropping is introduced by Gong *et al.* [4], and brings improvements for both image recognition and retrieval tasks. Scaling (high resolution inputs) improves performance in image retrieval tasks [21,22] where results with inputs at a resolution of 1,024 are better than results with images at lower resolutions such as 512 and 256. Other types of data augmentation techniques such as

rotation [23,24,25], translation [23,24,25], color shifting [23,26] and random noise [25] are also used at test-time for recognition and semantic segmentation tasks. To the best of our knowledge, all these test-time data augmentation approaches are introduced in a heuristic manner.

In this work, we seek to learn an optimal test-time data augmentation policy through reinforcement learning. Similar approaches have been proposed for image recognition tasks to learn the optimal train-time data augmentation, but not test-time augmentation. Cubuk *et al.* [14] applied a reinforcement learning method to find the best data augmentation policy. However, it is computationally infeasible for users with limited computational resources. Ho *et al.* [27] proposed a more efficient method using population-based training. Lim *et al.* [28] proposed a more efficient searching strategy based on density matching. Our work applies a similar searching strategy to that of Cubuk *et al.*, but our method reduces the computational cost caused by repeated inference stages through caching.

3 Proposed Method

In the following section, we first illustrate how to generate augmented features with a learned ensemble of test-time augmentations (TTA), and then describe how an optimal ensemble of TTA is learned.

Building Robust Feature from an Ensemble of TTA An augmented feature $\hat{\mathbf{f}}(I)$ for image I is generated by aggregating features extracted from transformed variants of I . The features used for aggregation are extracted using the following feature extraction protocol used in the recent studies of [21,22,29]. Consider $f_i(I)$ to be the extracted features from the i th layer of a CNN when I is the input image. The i th layer can be a convolutional or fully-connected layer. If the i th layer is a convolutional layer, $f_i(I)$ is a 3D tensor of width W , height H , and channels C . The extracted feature is transformed into a 1D vector by reshaping or aggregating. Conventionally, an aggregation process such as channel-wise max pooling (MAC) [30] or sum pooling (SPoC) [21] is applied to $f_i(I)$ to obtain a compact feature. Further, post-processing operations such as PCA whitening and normalization are also applicable. In this work, aggregation, PCA whitening and L2 normalization are applied to the feature $f_i(I)$, to obtain $\hat{f}_i(I)$.

Let t_j represent the j th type of image transformation, and $T = \{t_j | 1 \leq j \leq n\}$ is an ensemble of n transformations. The ensemble of features $F^{(T)}$ extracted from image I by applying the transforms T is given by,

$$F^{(T)} = \{\hat{f}_i(t_j(I)) | 1 \leq j \leq n\}. \quad (1)$$

In this work, the final augmented feature $\hat{\mathbf{f}}(I)$ is generated through a sum aggregation of $F^{(T)}$,

$$\hat{\mathbf{f}}(I) = \sum F^{(T)} = \sum_{j=1}^n \hat{f}_i(t_j(I)). \quad (2)$$

Finally, $\hat{f}(I)$ is L2 normalized, and can be compared to other features using the Euclidean distance.

In this work, the feature extraction during training and inference follows the same aforementioned protocol. In our experiments, the last activation layer of the Conv5 block of VGG16 [19] is aggregated with MAC [1] and is used as training features. Note that the input image size is 224×224 for trademarks or 512×512 for landmarks, except for images transformed with the Resize operation.

Learning an Ensemble of Image Transformations Finding the best ensemble of image transformations for off-the-shelf feature augmentation can be formulated as a discrete search problem. Inspired from the work by Cubuk *et al.* [14], we apply a Reinforcement Learning to determine the optimal ensemble of TTA for the target image retrieval task. It finds the best policy, S , which includes N learned image transformations, and comprises the transformation operations and their corresponding magnitudes. A recurrent neural network (RNN) based controller is trained for sampling policies as each policy is a sequence. At each step, the RNN produces a decision with a softmax classifier and sends it to the next step as an input for the next decision. In total, the controller has $2N$ softmax predictions. The final sequence of decisions is evaluated with a pre-trained convolutional neural network. The evaluation score is used as the reward, R . The controller is updated with R , achieved by the policy, S . An overview of this process is given in Fig. 1.

Similar to Cubuk *et al.* [14], we used a collection of image transformations within in PIL¹, and add two new operations: Resize and Horizontal-flip, which are widely used test-time augmentations [18,19,21,22]. The ensemble of transformations includes the following 16 transformations: *Resize*, *Rotate*, *ShearX/Y*, *TranslateX/Y*, *AutoContrast*, *Invert*, *Equalize*, *Solarize*, *Posterize*, *Contrast*, *Color*, *Brightness*, *Sharpness* and *Horizontal-flip*. We used the same operation magnitude ranges suggested by [14], except for Resize and Rotate. The magnitude range of the Resize operations is from 64 to 352 (for trademarks), or from 256 to 896 (for landmarks). Note that the width and height of input images are set to be the same. The range of the Rotate operation is $-\pi$ to π radians. The range of magnitudes are discretized into 10 values. To this end, if we sample N image transformations, the search space would be $(16 \times 10)^N$. In this work, N is set to 8. The reward function is designed to help the controller find an ensemble of image transformations that will increase the invariance and distinctiveness of augmented features.

Distinctive features for image retrieval will keep similar images close and dissimilar images distant in the feature space. To this end, we applied the contrastive loss [31] in Equation 3, which is widely used for metric learning to measure the distinctiveness of features,

¹ <https://pillow.readthedocs.io/en/stable/>

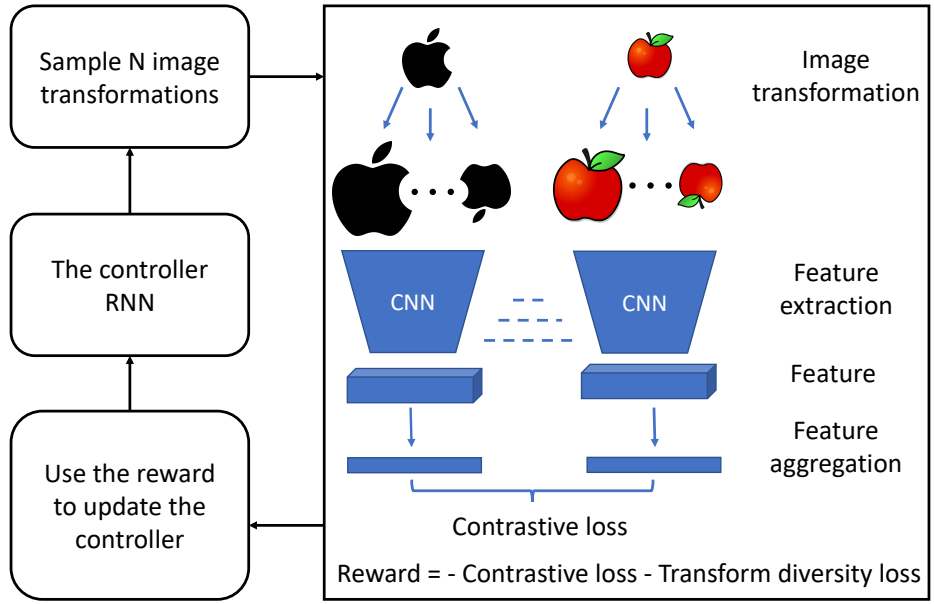


Fig. 1: The proposed scheme for searching for the optimal set of test-time data augmentations to enhance off-the-shelf CNN feature robustness for image retrieval. An RNN is used to search an ensemble of image transformations, and images are transformed with the selected transformations before feature extraction. Extracted features are aggregated (sum aggregation) and we calculate the contrastive loss. The reward is the negative sum of the contrastive loss, based on the similarity distances and the proposed transform diversity loss. Finally, the reward is used to update the controller.

$$L(f(i), f(j)) = \frac{1}{2} \|f(i) - f(j)\| * Y(i, j) + \frac{1}{2} \max\{0, \tau - \|f(i) - f(j)\|\} * Y(i, j), \tag{3}$$

where i and j are a pair of images. If they are similar, $Y(i, j)$ is 1, otherwise 0. τ is the margin, and is set to 0.7 in this work.

As shown in Fig. 1, augmented features are extracted for all similar and dissimilar image pairs from the training dataset with a Siamese network. The sum of contrastive loss, L_{Con} , is given by,

$$L_{Con} = \frac{1}{k} \sum_{i=1}^k L(\hat{\mathbf{f}}(I'_i), \hat{\mathbf{f}}(I''_i)), \tag{4}$$

where k is the batch size.

Generating features that offer multiple invariances is the main aim of this work. To this end, the ensemble of image transformations should be as diverse as possible. Additionally, we found an ensemble of diverse transformations is less

likely to overfit. To increase the diversity of an image transformation ensemble, we penalised the controller when the diversity of an ensemble is low. We calculated the *diversity loss* L_{Div} based on the number of unique image transformations $U(S)$ and the number of types of transform operations $T(S)$ in the policy S using,

$$L_{Div} = \alpha(1 - \frac{U(S)}{N}) + \beta(1 - \frac{T(S)}{N}), \quad (5)$$

where α and β are set to 0.2 and 0.025. When the policy S is composed of all unique transformations, L_{Div} is zero. When the policy S is made of one type of transformation, L_{Div} is close to $\alpha + \beta$.

The final reward R is equal to $-(L_{Con} + \lambda L_{Div})$, and λ is set to 1 in our experiments.

Accelerated Training via Caching Compared to other works *i.e.*, neural architecture search (NAS) [14,32], one iteration of the proposed method takes a comparatively very small amount of time as the feature extraction network is not trained. However, to further speed up the process, we cache features from previous iterations such that features are extracted only once for each transformation. This simple approach accelerates the whole training process by a factor of 100. With a GeForce GTX 1080 graphic card, a single training iteration takes around 3 – 5 seconds on our training dataset.

Training the Controller We optimised the controller with the Proximal Policy Optimisation algorithm [33], inspired by [14,32]. The controller is a one-layer LSTM [34] with 100 hidden units and $2 \times N$ softmax predictions for transformations and their corresponding magnitudes. The controller is trained with a learning rate of 10^{-5} . In total, the controller samples about 20,000 policies (the mode converges before 20,000 steps). The policy which achieves the highest reward is selected for inference.

4 Experiment

We tested the proposed method on both trademark and landmark image retrieval tasks, which are challenging and well-known content-based image retrieval tasks. In the following sub-sections, we present the datasets used, evaluation metrics, experimental setups and results.

4.1 Datasets

We selected the NPU trademark dataset [35] as the training dataset, and the METU dataset [15] as the testing dataset for trademark image retrieval. NPU is a small dataset that includes 317 similar trademark groups and each group contains at least two similar trademarks. In comparison, the METU trademark dataset includes nearly 1 million trademarks. The NPU dataset is used for generating training data, while the METU data is used for testing. As contrastive loss is applied in training, the training data is reorganised into similar and dissimilar

pairs. In total, 3,237 similar pairs are created by grouping any two images in the same group and the same amount of dissimilar pairs by grouping two random images from two different groups in the NPU dataset. Example similar and dissimilar pairs are shown in (a-b) and (e-f) of Fig. 2.

Similarly, a small subset of Google Landmark Dataset [36] is used for training, and Oxford5k [16] and Paris6k Datasets [17] are selected for testing the landmark retrieval task. The Oxford5k dataset includes 5,062 images (includes 55 queries), and the Paris6k dataset has 6,412 images (includes 55 queries). Similar and dissimilar pairs are also generated for training. We build similar pairs by grouping two randomly selected images from the most frequently appearing 2,442 landmarks in the Google Landmark dataset, and the same number of dissimilar pairs are created by grouping images belong to different landmark scenes. Example similar and dissimilar pairs are shown in (c-d) and (g-h) of Fig. 2.

4.2 Evaluation Metrics

We adopt the evaluation metric, *mean average precision* (MAP) in Equation 6, which is widely used in the related literature [15,22]. It is calculated using ranking positions obtained by sorting the image to query similarity distance in descending order. Note the MAP value is calculated using the top 100 ranking results for the METU trademark dataset, while for both Oxford5k and Paris6k datasets MAP is calculated from all images.

$$MAP@K = \frac{1}{Q} \sum_{i=1}^Q \frac{1}{E_i} \sum_j^k \frac{c_j}{j}, \quad (6)$$

where Q is the number of queries, and E_i is the number of expected results of the query i . r_j is one when image with rank j is the expected image, otherwise zero.

4.3 Experiment Setups

Images are resized before being passed to the networks for feature extraction. All trademark images from the METU dataset are resized 224×224 , and all landmark images from Oxford5k and Paris6k datasets are resized to 512×512 . To keep the original aspect ratio of the input image, a reflect padding is applied before resizing. In all experiments, full queries are used.

4.4 Results and Analysis

We selected the policy with the highest reward from all policies sampled by the controller on training datasets for our evaluation and ablation studies. The policy learned for trademarks on the NPU dataset is: *TranslateX: 1, Brightness: 1, ShearX: 1, Rotate: 10, TranslateY: 1, Resize: 1, Equalize: 1, Solarize: 3*, and the policy learned on the sub-set of Google landmark dataset for landmark



Fig. 2: Examples of similar and dissimilar pairs from METU trademark and Google landmark datasets. (a-d) are similar pairs, while (e-h) are dissimilar pairs.

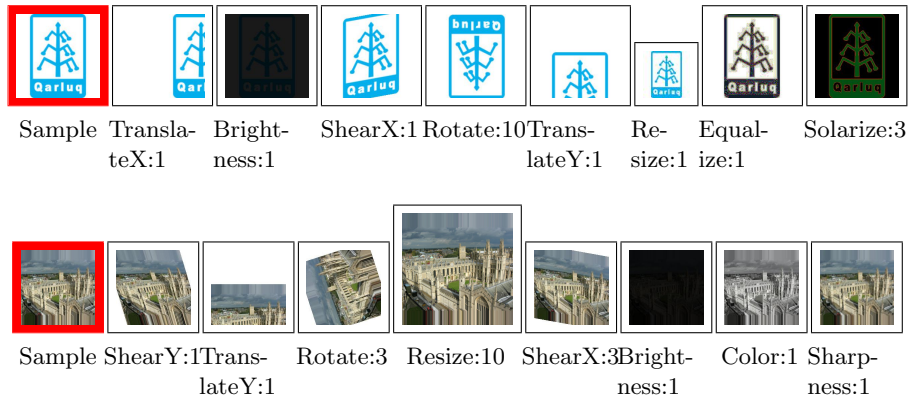


Fig. 3: Visualisation of the learned ensemble of TTA (*with* the diversity loss) with a sample image. Under each transformed image, the applied image transformation and magnitude are given. The top row shows the ensemble for trademark retrieval, while the bottom row shows the ensemble for landmark retrieval. Note that the resize operation shows only an approximate transform in consideration of the page limit and figure readability.

images is: *ShearY: 1, TranslateY:1, Rotate: 3, Resize: 10, ShearX: 3, Brightness: 1, Color: 1, Sharpness: 1*. The visualised policies with a sample image are shown in Fig. 3. The controller has learned two different policies for two different tasks.

Network Transferability We tested the learned policies with several ImageNet pre-trained networks including VGG16 [19], ResNet [5], DenseNet121 [37] and AlexNet [18]. All pre-trained models are from TorchVision ², except for

² <https://pytorch.org/docs/stable/torchvision/models.html>

VGG16 which is from Caffe model zoo ³. The feature extraction layers and results are shown in Fig. 4. With the learned TTA, all MAP results have increased. The improvement on both Oxford and Paris6k datasets are significant, and the improvement on METU data is not marginal as it is a very large-scale challenging dataset. We note that networks with skip-connections such as ResNet50 and DenseNet121 have higher improvements than convolutional networks without such connections. This may be due to the changes in the inputs sent to the deep layers via skip-connections.

Aggregation Transferability Here, we tested the learned policy with other types of aggregation methods, namely SPoC [21], GeM [22], CRoW [29] and R-MAC [12]. Features extracted from the last activation layer of Conv5 of VGG16 are used for implementing these aggregation methods. Hyper-parameters used in these methods are similar to those in [22], except for R-MAC. The scale factor of R-MAC is set to two, as a larger scale factor hurts its performance with the proposed method.

From the results shown in Fig. 5, we can see MAP results of all aggregation methods are improved. This shows the learned TTA is transferable to other aggregation methods. Nevertheless, we noticed MAC pooling achieves the largest improvement compared to other aggregations. A further improvement might be achievable for other aggregations if the same type of aggregation is applied during training and testing, as is the case for MAC aggregation.

Diversity loss The diversity loss is introduced to increase the generalization of the learned TTA, as a less diverse TTA has a higher chance to overfit on the training dataset. We compared the distribution of transformations of 100 unique policies with the highest rewards. The statistics are shown in Fig. 6 (policies learned *with* diversity loss) and 7 (policies learned *without* diversity loss). As we expected, the diversity loss increases the diversity of the learned TTA. With the diversity loss, learned policies are composed of more diverse transformations than the policies learned without it. For example, with diversity loss, around 10 among 16 operations frequently appear in the top rewarded policies. On the other hand, without diversity loss, only 3 among 16 operations appear on the top rewarded policies for trademark retrieval, and six operations for landmark retrieval. In addition, the best TTA without the diversity loss has less transformations compared to with the best TTA with diversity loss. For example, the best TTA learned without diverse loss for trademark retrieval task is: *Solarize: 1, Resize: 1, Resize: 1, Resize: 10, Rotate: 10, Rotate: 9, Rotate: 2, Solarize: 2*, and for landmark retrieval is: *TranslateX: 2, TranslateY: 2, TranslateY: 1, TranslateY: 1, Resize: 1, Solarize: 1, Rotate: 1, Rotate: 8*.

We also compared the best policies with/without the diversity loss with different pre-trained networks on three different datasets. The results are shown in Table 1. The best TTA learned the with diversity loss achieves higher MAP@100 scores on the METU trademark dataset compared to the TTA without the diversity loss. On the contrary, on the Oxford5k and Paris6k datasets the opposite is true. We suspect this may be due to the small number of transforms within the

³ https://caffe.berkeleyvision.org/model_zoo.html

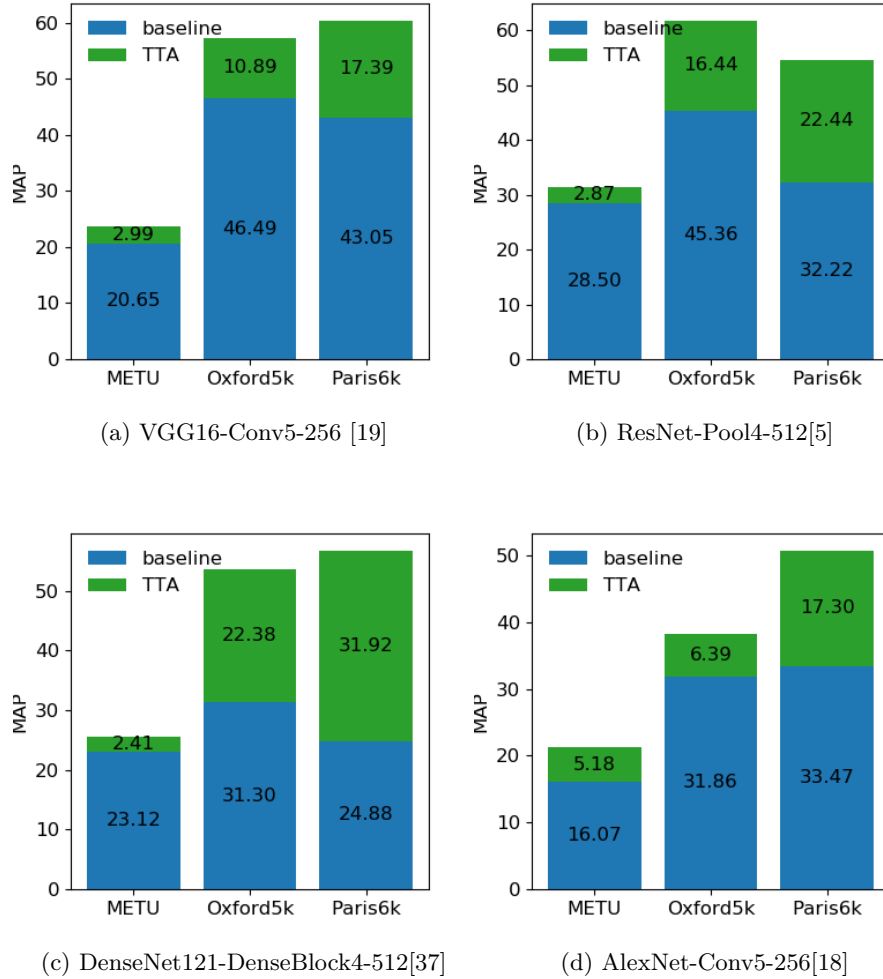
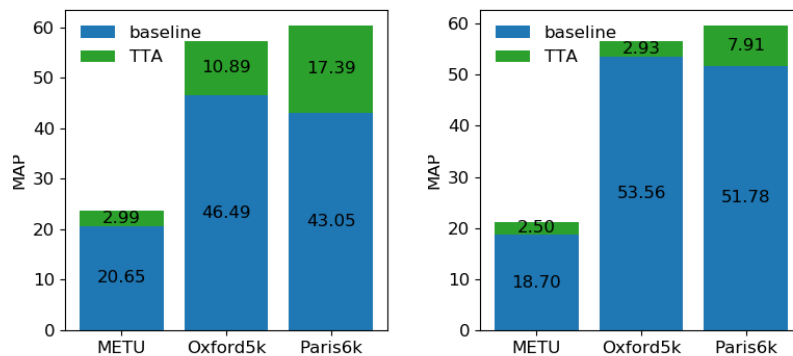
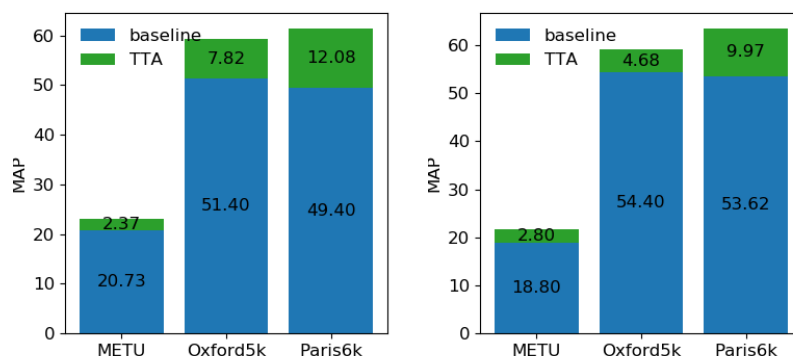


Fig. 4: Results for METU, Oxford5k and Paris6k datasets with off-the-shelf features from ImageNet pre-trained models with/without the learned ensemble of TTA. Sub-captions includes the network name, the feature extraction layer and the feature size. Note MAC pooling and PCA whitening are applied in all feature extraction processes.



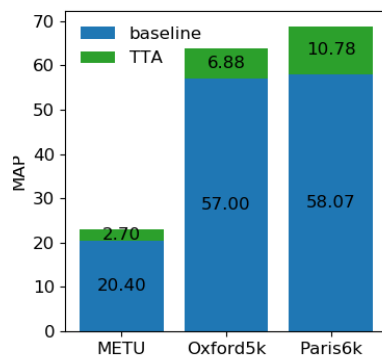
(a) MAC [30]

(b) SPoC [21]



(c) GeM [22]

(d) CRoW [29]



(e) R-MAC [12]

Fig. 5: Results for METU, Oxford5k and Paris6k datasets with aggregated VGG16/Conv5 off-the-shelf features with/without the learned ensemble of TTA. The used aggregation type is given in the sub-caption. Note all feature are resized to 256 after PCA whitening.

TTA and the high level of scale and location variation present in the landmark retrieval task compared to trademark retrieval.

Useful Image Transformations *Resize* and *Rotate* operations are the most frequently occurring image transformations for both trademark and landmark datasets. With these transformations, the augmented features gain certain scale and rotation invariance. On the contrary, *AutoContrast*, *Posterize*, *Invert* and *Horizontal-flip* operations rarely appear in both datasets. *Solarize*, *Equalize* and *Contrast* operations frequently appear in the trademark retrieval task because of domain variance in the trademark datasets. In contrast, *Sharpness* and *Color* operations has a higher occurrence rate in the Landmark retrieval task.

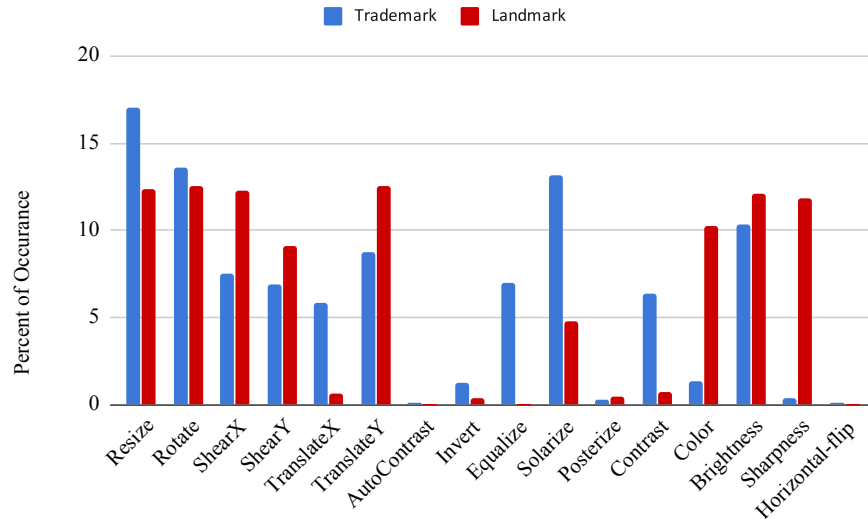


Fig. 6: The rate of occurrence of image transformations in sampled unique policies (learned *with* the diversity loss) with the top 100 rewards on NPU trademark and Google landmark datasets.

Comparison with State-of-the-art Results In this work, we achieved state-of-the-art (SOTA) MAP@100 results on the METU trademark dataset as show in Table 2. Our best result is based on ResNet50/Pool4 MAC features extracted with the learned TTA. It achieves a MAP@100 score of 31.37. A qualitative comparison with the previous SOTA on two challenging queries is show in Fig. 8. Note that without the TTA, VGG16/Pool4 R-MAC and ResNet50/Pool4 MAC features achieved a MAP@100 scores of 27.1 and 28.5, which also surpass previous SOTA results. However, this demonstrates our method is also valid when applied to already high performing features.

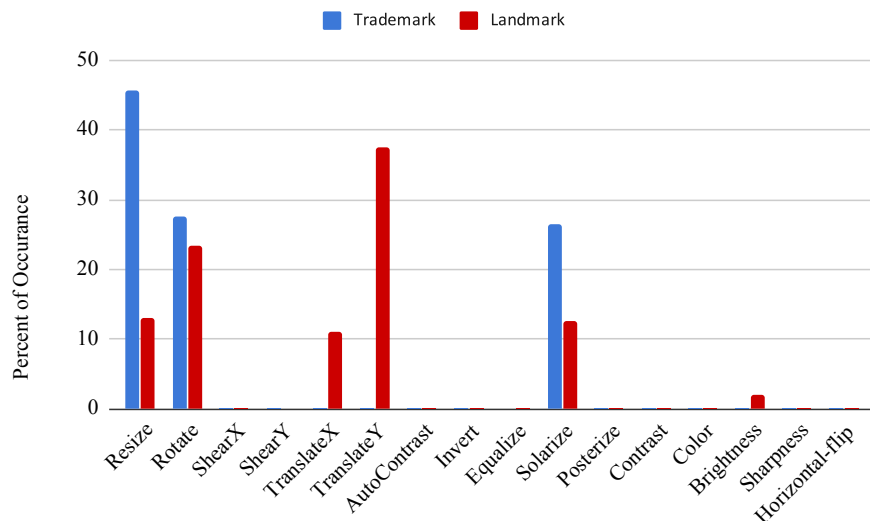


Fig. 7: The rate of occurrence of image transformations in sampled unique policies (learned *without* the diversity loss) with the top 100 rewards on NPU trademark and Google landmark datasets.

Table 1: Comparisons of the ensembles of TTA learned with/without the diversity loss. Results are highlighted in **bold** if improved.

Networks	Layer	Dim	Diversity Loss	METU	Oxford5k	Paris6k
				MAP@100 ↑	MAP ↑	MAP ↑
VGG16 [19]	Conv5	256	-	22.91	60.52	76.03
			✓	23.64	57.38	60.44
ResNet5 [5]	Pool4	512	-	27.3	62.2	75.06
			✓	31.37	61.8	54.66
DenseNet121 [37]	DenseBlock4	512	-	24.93	56.19	75.09
			✓	25.53	53.68	56.80
AlexNet [18]	Conv5	256	-	19.78	47.47	67.27
			✓	21.25	38.25	50.77

Weaknesses and Suggested Improvements The learned ensemble of TTA has shown improvements on both trademark and landmark retrieval tasks, though we observe numerous avenues for improvements. As such, we highlight several modifications that may introduce further improvements. First, the transformations themselves can be better targeted at the dataset domains. The image transformations used here are proposed for image classification tasks and are thus potentially not optimal. Second, naive sum aggregation is used for merg-

Table 2: Comparison with the previous state-of-the-art results on METU dataset.

	Method	TTA	DIM↓	MAP@100 ↑
Baseline	ATR R-MAC [2]		256	25.7
	ATR CAM MAC [2]		512	25.1
Ours	ResNet50/POOL4 MAC	✓	512	28.5
			512	31.37
	VGG16/POOL4 R-MAC	✓	256	27.9



Fig. 8: Comparison of top 10 results of our best method (ResNet50/Pool4 MAC with TTA) and the previous state-of-the-art method (ATR MAC) on the METU trademark dataset. For each query, the second row is our result, and positive results are noted with a green box.

ing TTA features. Alternatives such as max and VLAD [38] can be replaced. Third, the number of transformations and the number of magnitudes can be increased. Fourth, Training datasets are small, and generated randomly (especially for landmark tasks). Large and clean training datasets will be beneficial. Finally, a more advanced training loss *i.e.* Triplet loss [39] and better controller design are also likely to be effective and worth investigating.

5 Conclusion

In this work, we applied a reinforcement learning approach to learn an ensemble of test-time data augmentations to enhance feature invariance for image retrieval in a computationally efficient and affordable manner. We proposed a reward function to increase invariance and distinctiveness of the features aggregated from the learned transformations. The proposed method not only improves the performance of off-the-shelf features used in the training stage, but it also demonstrates transferability to features extracted with different networks and feature aggregation methods.

References

1. Sharif Razavian, A., Azizpour, H., Sullivan, J., Carlsson, S.: Cnn features off-the-shelf: an astounding baseline for recognition. In: Proceedings of the IEEE conference on computer vision and pattern recognition workshops (CVPRW). (2014)
2. Tursun, O., Denman, S., Sivapalan, S., Sridharan, S., Fookes, C., Mau, S.: Component-based attention for large-scale trademark retrieval. *IEEE Transactions on Information Forensics and Security (TIFS)* (2019)
3. Aker, C., Tursun, O., Kalkan, S.: Analyzing deep features for trademark retrieval. In: *Signal Processing and Communications Applications Conference (SIU)*. (2017)
4. Gong, Y., Wang, L., Guo, R., Lazebnik, S.: Multi-scale orderless pooling of deep convolutional activation features. In: *European conference on computer vision (ECCV)*. (2014)
5. He, K., Zhang, X., Ren, S., Sun, J.: Deep residual learning for image recognition. *arXiv preprint arXiv:1512.03385* (2015)
6. Jaderberg, M., Simonyan, K., Zisserman, A., et al.: Spatial transformer networks. In: *Advances in neural information processing systems (NeurIPS)*. (2015)
7. Hinton, G.E., Krizhevsky, A., Wang, S.D.: Transforming auto-encoders. In: *International conference on artificial neural networks (ICANN)*. (2011)
8. Ciregan, D., Meier, U., Schmidhuber, J.: Multi-column deep neural networks for image classification. In: *IEEE conference on computer vision and pattern recognition (CVPR)*. (2012)
9. Dai, J., Qi, H., Xiong, Y., Li, Y., Zhang, G., Hu, H., Wei, Y.: Deformable convolutional networks. In: *ICCV*. (2017)
10. Marcos, D., Volpi, M., Tuia, D.: Learning rotation invariant convolutional filters for texture classification. In: *International Conference on Pattern Recognition (ICPR)*. (2016)
11. Follmann, P., Bottger, T.: A rotationally-invariant convolution module by feature map back-rotation. In: *IEEE Winter Conference on Applications of Computer Vision (WACV)*. (2018)
12. Toliás, G., Sicre, R., Jégou, H.: Particular object retrieval with integral max-pooling of cnn activations. *arXiv preprint arXiv:1511.05879* (2015)
13. Zoph, B., Le, Q.V.: Neural architecture search with reinforcement learning. *arXiv preprint arXiv:1611.01578* (2016)
14. Cubuk, E.D., Zoph, B., Mane, D., Vasudevan, V., Le, Q.V.: Autoaugment: Learning augmentation strategies from data. In: *Proceedings of the IEEE conference on computer vision and pattern recognition (CVPR)*. (2019) 113–123
15. Tursun, O., Aker, C., Kalkan, S.: A large-scale dataset and benchmark for similar trademark retrieval. *CoRR* (2017)
16. Philbin, J., Chum, O., Isard, M., Sivic, J., Zisserman, A.: Object retrieval with large vocabularies and fast spatial matching. In: *Proceedings of the IEEE Conference on Computer Vision and Pattern Recognition (CVPR)*. (2007)
17. Philbin, J., Chum, O., Isard, M., Sivic, J., Zisserman, A.: Lost in quantization: Improving particular object retrieval in large scale image databases. In: *2008 IEEE conference on computer vision and pattern recognition (CVPR)*, IEEE (2008) 1–8
18. Krizhevsky, A., Sutskever, I., Hinton, G.E.: Imagenet classification with deep convolutional neural networks. In: *Advances in neural information processing systems (NeurIPS)*. (2012)
19. Simonyan, K., Zisserman, A.: Very deep convolutional networks for large-scale image recognition. *arXiv preprint arXiv:1409.1556* (2014)

20. Szegedy, C., Liu, W., Jia, Y., Sermanet, P., Reed, S., Anguelov, D., Erhan, D., Vanhoucke, V., Rabinovich, A.: Going deeper with convolutions. In: Proceedings of the IEEE conference on computer vision and pattern recognition (CVPR). (2015) 1–9
21. Babenko, A., Lempitsky, V.: Aggregating local deep features for image retrieval. In: Proceedings of the IEEE international conference on computer vision (ICCV). (2015)
22. Radenović, F., Tolias, G., Chum, O.: Fine-tuning cnn image retrieval with no human annotation. *IEEE transactions on pattern analysis and machine intelligence (PAMI)* (2018)
23. Perez, F., Vasconcelos, C., Avila, S., Valle, E.: Data augmentation for skin lesion analysis. In: *OR 2.0 Context-Aware Operating Theaters, Computer Assisted Robotic Endoscopy, Clinical Image-Based Procedures, and Skin Image Analysis*. Springer (2018) 303–311
24. Matsunaga, K., Hamada, A., Minagawa, A., Koga, H.: Image classification of melanoma, nevus and seborrheic keratosis by deep neural network ensemble. *arXiv preprint arXiv:1703.03108* (2017)
25. Wang, G., Li, W., Aertsen, M., Deprest, J., Ourselin, S., Vercauteren, T.: Test-time augmentation with uncertainty estimation for deep learning-based medical image segmentation. (2018)
26. Nalepa, J., Myller, M., Kawulok, M.: Training-and test-time data augmentation for hyperspectral image segmentation. *IEEE Geoscience and Remote Sensing Letters* **17** (2019) 292–296
27. Ho, D., Liang, E., Chen, X., Stoica, I., Abbeel, P.: Population based augmentation: Efficient learning of augmentation policy schedules. In: *International Conference on Machine Learning (ICML)*. (2019) 2731–2741
28. Lim, S., Kim, I., Kim, T., Kim, C., Kim, S.: Fast autoaugment. In: *Advances in Neural Information Processing Systems (NeurIPS)*. (2019)
29. Kalantidis, Y., Mellina, C., Osindero, S.: Cross-dimensional weighting for aggregated deep convolutional features. In: *European conference on computer vision (ECCV)*. (2016)
30. Azizpour, H., Sharif Razavian, A., Sullivan, J., Maki, A., Carlsson, S.: From generic to specific deep representations for visual recognition. In: *Proceedings of the IEEE conference on computer vision and pattern recognition workshops (CVPRW)*. (2015)
31. Chopra, S., Hadsell, R., LeCun, Y.: Learning a similarity metric discriminatively, with application to face verification. In: *Proceedings of the IEEE Conference on Computer Vision and Pattern Recognition (CVPR)*. (2005)
32. Zoph, B., Vasudevan, V., Shlens, J., Le, Q.V.: Learning transferable architectures for scalable image recognition. In: *Proceedings of the IEEE Conference on Computer Vision and Pattern Recognition (CVPR)*. (2018)
33. Schulman, J., Wolski, F., Dhariwal, P., Radford, A., Klimov, O.: Proximal policy optimization algorithms. *arXiv preprint arXiv:1707.06347* (2017)
34. Hochreiter, S., Schmidhuber, J.: Long short-term memory. *Neural computation* (1997)
35. Lan, T., Feng, X., Xia, Z., Pan, S., Peng, J.: Similar trademark image retrieval integrating lbp and convolutional neural network. In: *International Conference on Image and Graphics (ICIGP)*. (2017)
36. Noh, H., Araujo, A., Sim, J., Weyand, T., Han, B.: Large-scale image retrieval with attentive deep local features. In: *Proceedings of the IEEE international conference on computer vision (ICCV)*. (2017) 3456–3465

37. Huang, G., Liu, Z., van der Maaten, L., Weinberger, K.Q.: Densely connected convolutional networks. In: Proceedings of the IEEE Conference on Computer Vision and Pattern Recognition (CVPR). (2017)
38. Arandjelovic, R., Zisserman, A.: All about vlad. In: Proceedings of the IEEE conference on Computer Vision and Pattern Recognition (CVPR). (2013) 1578–1585
39. Schroff, F., Kalenichenko, D., Philbin, J.: Facenet: A unified embedding for face recognition and clustering. In: Proceedings of the IEEE conference on computer vision and pattern recognition (CVPR). (2015) 815–823